2020 American Control Conference
Denver, CO, USA, July 1-3, 2020

Optimal Operation of a Plug-in Hybrid Vehicle with Battery Thermal and Degradation Model

Jongho Kim[1,*] Youngsuk Park[1] John D. Fox[2] Stephen P. Boyd[1] William Dally[3]

***Abstract*— We propose a control method to optimally use fuel and battery resources for power-split plug-in hybrid vehicles (PHEVs) under the case of pre determined driving route and associated energy demand profile. We integrate a battery thermal and degradation model and formulate a mixed-integer convex problem which can be approximately solved with standard efficient solvers. In simulation, we demonstrate that our controller can manage battery operation and state to avoid severe battery degradation, and balance fuel usage with battery degradation depending on ambient temperature or energy demand profiles of the routes. Under various scenarios, the results are validated by the Autonomie software [1] and compared with conventional existing CDCS controller and the earlier related work [2], which only optimized to achieve minimal fuel use and neglects the battery degradation. Lastly, we show our controller is efficient enough to be computed on the on-board vehicle computer and applied in real-time.**

I. INTRODUCTION

A. Motivation

Development of Electric vehicles (EVs), hybrid and plug-in hybrid vehicles (PHEVs) is an active research area for next-generation vehicles. The market share of hybrid and PHEVs is estimated to reach 30% by 2050 and growing demands of both EVs and PHEVs are expected [3]. PHEVs in particular have an interesting control problem since they all possess a special combined energy system of electricity and gasoline along with internal controllers capable of shifting energy resources. Studies ([4], [5], [6]) have shown that the choice of internal energy resource during the route can have substantial impacts on the overall vehicle efficiency and thereby highlight the importance of PHEV control strategies.

Several control strategies for PHEVs have been proposed, analysed and validated through numerical experiments. A simple, yet the most common strategy is the *Charge-Depletion Charge Sustaining* (CDCS) controller which starts a trip with a near fully-charged battery and runs on the electric motor until the battery is discharged to a certain threshold (*i.e.*, Charge-depleting mode). After this point on a trip, it operates both electric motor and fuel engine, charges the battery and maintains a nominal charge level (*i.e.*, Charge-sustaining mode). Another well-known control strategy is *blend mode* which is a table-based (or empirically) method that uses both motor and the engine based on the assumption that the total trip length (*i.e.*, driving range) is known [7]. While existing controllers are simple and effective in special cases, they are naive in a sense that they do not extensively consider the battery degradation effect and the efficient balancing of both the ICE and the battery during trips. Because the economic cost of the battery resource is significant, operational strategies that extend the service life of the battery are of great practical value.

Battery degradation models ([8], [9], [10]) have been proposed along with empirical validation. However, most models are presented in non-formulated forms and are not practically applicable for an on-board vehicle implementation due to model complexity. For example, Wang et al. [11] propose a model which does not depend on the input current when the current is less than half of the absolute value of current rate (*i.e.*, $C/2$) while Zabala et al. [9] propose a model which defines the input current as a main dependent variable.

This paper is focused on finding a control strategy which simultaneously optimizes the battery and fuel usage on power-split PHEVs based on the prior knowledge of a route energy demand profile. We assume that this prior route information (including energy demand profile) is fully determined and consider a simple yet practical battery degradation model. The prior route information could be from well-trained statistical estimation models of prior routes or accurate GPS data measurements, which is out of our focus of this paper, though interesting as a separate research topic. The techniques from this paper are generally applicable along with many efficient route prediction methods. We use (mixed integer) convex optimization to obtain the efficient optimal control strategy.

B. Contributions

- We consider a control problem that minimize the fuel efficiency and battery degradation of PHEVs with vehicle dynamic constraints, the battery thermal model and a degradation model.
- We propose a tractable formulation via convex relaxation on non-convex terms, which leads to scalable algorithms.
- Numerical experiments demonstrate that our method can manage the battery for less degradation whereas other controllers (*e.g.*, CDCS and the controller on our earlier work [2]) cannot.

C. Outline

The paper is organized as follows: in Section II, general backgrounds for the battery model and our PHEV model are introduced; in Section III, we formulate an optimal control problem under pre-determined route profile and transform

*Corresponding author
[1]Department of Electrical Engineering, Stanford USA.
[2]Department of Applied Physics, Stanford USA.
[3]Department of Computer Science, Stanford USA.

978-1-5386-8266-1/$31.00 ©2020 AACC

this into an approximated convex optimization problem; in Section IV, we compare our optimal controller to other existing controllers via numerical experiments, showing the effectiveness of our method. Lastly, in Section V conclusions and future research directions are discussed.

II. Background

We explain our hybrid vehicle model and battery models. We consider the time horizon $t \in [0,T]$ where T denotes the arrival time (*i.e.*, end of a trip). As mentioned, the required vehicle speed and the desired drive power $P_{\text{des}}(t) \in \mathbf{R}$ over the route are assumed to be known based on precise route estimation models or can be obtained from past history.

A. Drivetrain

We consider a Power-Split PHEV which can be found in cars such as Toyota Prius. This kind of drivetrain uses two on-board energy sources, fuel $P_{\text{fuel}}(t) \in \mathbf{R}$ and battery $P_b(t) \in \mathbf{R}$. The drivetrain combines these available powers to output desired power $P_{\text{des}}(t) \in \mathbf{R}$. We regard $P_b(t) > 0$ as power extracted from the battery and $P_b(t) < 0$ as power re-charged to the battery. For all $t \in [0,T]$, battery energy has a power limit, *i.e.*,

$$P_b^{\min} \leq P_b(t) \leq P_b^{\max}. \tag{1}$$

And $P_{\text{fuel}}(t) \geq 0$ since fuel energy does not directly return or be re-charged.

Our Controllers must operate a drivetrain to produce the target power $P_{\text{des}}(t)$ for every time $t \in [0,T]$. To attain this target power, every power-split drivetrain uses a converter that allows dynamic selections between two different modes $\theta(t) \in \{0,1\}$ at time t as follows

$$\begin{aligned} P_{\text{des}}(t) &= f_\theta\left(P_{\text{fuel}}(t), P_b(t)\right) \\ &= \begin{cases} P_b(t) & \theta(t) = 0 \\ f(P_{\text{fuel}}(t), P_b(t)) & \theta(t) = 1 \end{cases}. \end{aligned} \tag{2}$$

Here at mode $\theta(t) = 0$, engine is off and thus all power comes from the battery only. At mode $\theta(t) = 1$, drive power comes from both engine and battery, as a function of P_{fuel} and P_b. We assume the function $f : \mathbf{R} \times \mathbf{R} \mapsto \mathbf{R}$ is *increasing* in each argument and *concave*, even though f often does not have a closed form. Although these theoretical assumptions are not always guaranteed in practice, our method can be used with a good approximated function $\hat{f}$ that is close to f. Using these assumptions, we can represent P_{fuel} as a function of P_b and P_{des}, *i.e.*,

$$\begin{aligned} P_{\text{fuel}}(t) &= h_\theta(P_b(t), P_{\text{des}}) \\ &= \begin{cases} 0 & \theta(t) = 0 \\ h(P_b(t), P_{\text{des}}) & \theta(t) = 1 \end{cases} \end{aligned}$$

Note that given P_{des}, h is decreasing and convex in P_{b}. To obtain a control strategy which minimizes P_{fuel} over time, it is important to represent h in a tractable form. In most practical cases, closed form of h is not readily available. Here, we use a simple gridding method to represent h approximately. For detailed definitions and explanations, please refer to V and our previous paper [2] on representing h for Power-Split PHEVs and the justification of this approach.

B. Battery

There exist many equivalent circuit models describing battery dynamics and in this work we adopt a very simple RC equivalent circuit [2]. The battery model is an RC finite reservoir with a finite total energy capacity $C_{\text{b}} \in \mathbf{R}$, a nominal voltage $V \in \mathbf{R}$, and internal resistance $R_{\text{int}} \in \mathbf{R}$. Note that these quantities depend on the specific type and technology of the battery.

a) Battery Power loss: Battery losses are determined as P^2 loss term which penalizes large withdrawals of battery power in short amounts of time. In our model, if we require a certain amount power P_e to run the motors, the power P_b withdrawn from the battery is

$$P_b = \left(P_e + \tfrac{1}{2} P_e^2 \tfrac{R_{\text{int}}}{V^2}\right) / P_{\text{eff}} \tag{3}$$

where $P_{\text{eff}} \in \mathbf{R}$ is the efficiency of power converters. The analogous expression is used for expressing losses while charging the battery.

b) Battery Energy: We assume the initial battery energy $E_b(0)$ is known and fixed:

$$E_b(0) = E_b^{\text{init}} \tag{4}$$

with $E_b^{\text{init}} \in \mathbf{R}$ with unit of Joules. The energy drawn from battery is

$$\dot{E}_b(t) = -P_b(t) \tag{5}$$

c) Battery Thermal Model: Battery temperature during operations may greatly affect performances, life, and reliability of the battery system [10]. The heat generation in batteries are from two major sources: 1) electrochemical operation and 2) Joule heating. Thermal modeling of battery relies heavily on the fundamental of heat transfer [12]. Deriving a perfectly precise model for heat transfer is challenging due to the complexity of battery chemistry and material compositions [13]. In this work, we adopt a simple heat transfer model as follows

$$mC\dot{T}_b(t) = |P_b(t)| + h_{\text{trans}}\left(T_b(t) - T_{\text{amb}}(t)\right) \tag{6}$$

Here, for a battery $m \in \mathbf{R}$ is its total mass, $C \in \mathbf{R}$ is its heat capacity, $h_{\text{trans}} \in \mathbf{R}$ is its heat transfer coefficient. $T_{\text{amb}} \in \mathbf{R}$ is ambient temperature (*i.e.*, 298K) which is assumed to be fixed over time $[0,T]$ and $T_b \in \mathbf{R}$ is the battery temperature at time t. Note that C depends on composition and chemistry of batteries and h_{trans} may also reflect the efficiency of battery cooling system in PHEVs. Please refer to appendix V for detailed specifications. In this work, we set the initial battery temperature as the ambient temperature at our departure location. (*i.e.*, $T_b(0) = T_{\text{amb}}$).

d) Battery Degradation Model: Battery degradation is caused by the structural and chemical transformations such as electrolyte oxidation at the cathode and growth of solid electrolyte interface on the anode [14]. Two kinds of battery degradation effects have been studied in literature ([15], [11], [9]): 1) calendar aging (without using battery) and 2)

cyclic aging (using battery). Calendar aging is dependent on temperature and state-of-charge (SOC) which are coupled with an Arrhenius relationship which results in an underlying dependency on time (t^z) where z tends to be $1/2$. Cycling aging is dependent on temperature, charge/discharge current and total charge/discharge delivered which is often referred as ampere hour throughput $Ah_t = \int_{\tau=0}^{t} |I_b(\tau)| d\tau$.

Here, we regard the cyclic aging effect as a main cause of battery degradation since we consider relatively short time horizon T. Let $Q_d(t) \in \mathbf{R}$ be the cumulative degradation or loss of capacity so far and $\dot{Q}_d(t) \in \mathbf{R}$ be the battery degradation rate at time t. The simple culmulaative degradation model on PHEV battery has been suggested by Ahmadian et al. [13] and we derive the degradation rate version as follows

$$\dot{Q}_d(t) = c_1 \exp\left(\frac{c_2 + c_3 |I_b(t)|}{R_{\text{gas}} T_b}\right) \cdot g(Ah_t, I_b(t)) \tag{7}$$

where c_1, c_2, $c_3 \in \mathbf{R}_+$ are fitted constants varied by the types of battery and $R_{\text{gas}} = 8.314$ $[J \cdot \text{mol} \cdot K^{-1}]$ is gas constant. $I_b(t) \in \mathbf{R}$ is charging (positive) or discharging (negative) battery current and $P_b(t) = \text{sign}(I_b(t)) I_b^2(t) R_{\text{int}}$ is defined accordingly. Lastly, the degradation rate of Ah effect is $g(Ah_t, I_b(t)) = Ah_t^{z-1} |I(t)|$ where z depends on battery technology and type, and we consider $z = 0.5$.

This model expresses a degradation effect with respect to charging rates and battery temperature. More specifically, the model is able to capture the following degradation properties: 1) the rate of degradation is faster under high $|I_b(t)|$ (or C-rate), 2) the model follows *Arrhenius rule* of the chemical activity on temperature, *i.e.*, chemical reaction is faster under high temperature $T_b(t)$ and high current $I_b(t)$, 3) the speed of degradation depends on cumulative charge of battery delivered over time.

e) Internal Resistance of Battery: Gong et al. [10] showed the dependency of battery internal resistance on battery SOC and different temperatures. Particularly, under the fixed temperatrue, the internal resistance R_{int} is almost constant within 20% to 80% battery SOC range (Refer to Figure 3.11 [10]). The value depends on battery temperature with Arrenhius model but the value stays within approximately 1 m Ω to 3 mΩ within a moderate range of temperature.

III. Optimal Control

Our goal is to efficiently operate a drivetrain to meet the target power requirement $P_{\text{des}}(t)$ for time t over the finite time horizon $[0, T]$. Here, we design a tractable form of the objective function for total costs and constraints for engine and battery models, via convex relaxations.

A. Constraints

a) Battery Temperature: EVs and PHEVs must maintain the operating range of battery temperatures through control by cooling systems as temperatures outside the desired range may severely affect the battery performances [16]. We have modeled a finite capacity cooling system which regulates the battery temperature within a specific range of temperatures. By controlling the power dissipation in the battery, we keep the battery temperature within

$$T^{\min} \leq T_b(t) \leq T^{\max} \tag{8}$$

over time $t \in [0, T]$. We set the minimum temperature to be ambient (*i.e.*, $T^{\min} = T_{\text{amb}}$) and allow maximum temperature to be $45°C$ above the ambient temperature of $25°C$ (*i.e.*, 343 K).

b) Finite Battery Resource: The battery energy has limits

$$E^{\min} \leq E(t) \leq E^{\max} \tag{9}$$

for all $t \in [0, T]$. In other words, the controller only allows the operation within a fixed range of the battery SOC. This constraint is common to prevent a severe battery degradation and usually $E^{\min}$ is 20% and $E^{\max}$ is 80% of the total battery energy (*i.e.*, $E^{\min} = 0.2C$ and $E^{\max} = 0.8C$ where C here is battery capacity).

B. Cost Function

Our total cost function for operating the vehicle is a combination of four objectives

$$J = J_{\text{fuel}} + \lambda_1 J_{\text{cooling}} + \lambda_2 J_{\text{degrad}} + \lambda_3 S \tag{10}$$

where λ_1, λ_2, $\lambda_3 \geq 0$. We specify each of objectives below.

a) Fuel Cost: Total cost of fuel consumed $J_{\text{fuel}} \in \mathbf{R}$ is

$$J_{\text{fuel}} = (\pi \eta) \int_0^T P_{\text{fuel}}(t) dt. \tag{11}$$

where $\eta \in \mathbf{R}$ is the heating value of a fuel and $\pi \in \mathbf{R}$ is a fuel price. We assume that fuel price is fixed over time $t \in [0, T]$.

b) Switch Cost: We would like to minimize the number of times the fuel engine is turned on or off in operation, and once started, we should run the engine at an efficient operating temperature. Therefore, we introduce a switching cost $S = \int_{t=0}^{T} \mathbf{1}(\dot{\theta}(t) = 0) dt$ which is the number of times a mode $\theta(t)$ switches between $0, 1$.

c) Cooling Cost: In our vehicle model, we choose a simple battery cooling system and define the cost of power usage by battery cooling system as

$$J_{\text{cooling}} = \int_0^T h_{\text{trans}} \left(T_b(t) - T_{\text{amb}}\right) dt \tag{12}$$

where $h_{\text{trans}} \in \mathbf{R}$ is battery heat transfer coefficient defined in 6 and specified in II. This represents a passive cooling system which aims to set battery temperature to ambient temperature via a capacity limited heat transfer.

d) Degradation Cost: The cost of battery degradation is

$$J_{\text{degrad}} = \int_0^T \phi\left(\dot{Q}_d(t)\right) dt. \tag{13}$$

where $\phi : \mathbf{R} \mapsto \mathbf{R}$ is a non-negative and increasing cost function associated with the battery degradation rate. ϕ can be nonlinear and may not have a closed form expression, so we will use a tractable surrogate function in later section.

Notation	Definition
J_{fuel}	Total fuel usage cost
J_{cooling}	Total cooling power cost
J_{degrad}	Total battery degradation cost
S	Total switch cost
P_{fuel}	Fuel power
P_b	Battery power
P_{des}	Power demand
T_b	Battery temperature

TABLE I: Notations and parameters for optimization problem

C. Non-convex Problem

Therefore, the optimization problem is

$$\begin{aligned}
\text{minimize} \quad & J := J_{\text{fuel}} + \lambda_1 J_{\text{cooling}} + \lambda_2 J_{\text{degrad}} + \lambda_3 S \\
\text{subject to} \quad & P_{\text{fuel}}(t) = h_\theta(P_b(t), P_{\text{des}}(t)) \\
& \dot{E}(t) = -P_b(t) \\
& P_b^{\min} \le P_b(t) \le P_b^{\max} \\
& E^{\min} \le E(t) \le E^{\max} \\
& E(0) = E^{\text{init}} \\
& T_b(0) = T_{\text{amb}} \\
& T^{\min} \preceq T_b(t) \preceq T^{\max} \\
& mC\dot{T}_b(t) = |P_b(t)| - h_{\text{trans}}\left(T_b(t) - T_{\text{amb}}\right),
\end{aligned} \tag{14}$$

with variables $\theta(t) \in \{0,1\}$, $P_b(t) \in \mathbf{R}$, $T_b(t) \in \mathbf{R}_+$ and $E(t) \in \mathbf{R}_+$ over $t \in [0,T]$. In this problem, m, C, h_{trans} are defined by vehicle specifications and T_{amb}, $P_b^{\min}$, $P_b^{\max}$, $E^{\min}$, $E^{\max}$, $T^{\min}$ and $T^{\max}$ are model parameters we select (see Appendix V-B). Note that this is a mixed integer non-convex optimization problem for which no general algorithms is known to be efficient to solve.

D. Tractable Mixed-Integer Convex Problem via Relaxation

To solve (14) approximately, we convert it into the following mixed-integer convex problem.

$$\begin{aligned}
\text{minimize} \quad & J := J_{\text{fuel}} + \lambda_1 J_{\text{cooling}} + \lambda_2 \mathbf{J}_{\text{degrad}}^{\{\alpha\}} + \lambda_3 S \\
\text{subject to} \quad & P_{\text{fuel}}(t) = h_\theta(P_b(t), P_{\text{des}}(t)) \\
& \dot{E}(t) = -P_b(t) \\
& P_b^{\min} \le P_b(t) \le P_b^{\max} \\
& E^{\min} \le E(t) \le E^{\max} \\
& E(0) = E^{\text{init}} \\
& T_b(0) = T_{\text{amb}} \\
& T^{\min} \preceq T_b(t) \preceq T^{\max} \\
& \mathbf{mC\dot{T}_b(t)} \ge |\mathbf{P_b(t)}| - \mathbf{h}_{\text{trans}}\left(\mathbf{T_b(t)} - \mathbf{T}_{\text{amb}}\right),
\end{aligned} \tag{15}$$

with variables $\theta(t)$, $P_b(t)$, $T_b(t)$ and $E(t)$ over $t \in [0,T]$. Now we explain how to relax non-convex terms in (14) to (bold) convex ones above.

a) Relaxation on thermal model: Re-arranging the equation (6), we have

$$\dot{T}_b(t) = \left(|P_b(t)| - h_{\text{trans}}\left(T_b(t) - T_{\text{amb}}\right)\right)/mC.$$

Note that this is a non-affine equality constraint because the right hand side is a convex function for all $T_b \in \mathbf{R}$ and $P_b \in \mathbf{R}$. In order to preserve the convexity of the problem, we replace the constraint with

$$\dot{T}_b(t) \ge \left(|P_b(t)| - h_{\text{trans}}\left(T_b(t) - T_{\text{amb}}\right)\right)/mC. \tag{16}$$

Here, we relaxed this equality constraint into an inequality constraint. This relaxation is not tight in general, but is tight if the solution of original problem (14) satisfies $T_b(t) \ge T_{\text{amb}}$ over all time $t \in [0,T]$ and $\lambda_2 = 0$. To see this, note that J_{cooling} encourages temperature $T_b(t)$ as small as possible (provided $T_b(t) \ge T_{\text{amb}}$). In other words, among any feasible points satisfying inequality, the solution taken will be the smallest one $T_b(t)$ and $\dot{T}_b(t)$ accordingly (for given previous temperature $T_b(t-\Delta t)$), making this inequality tight.

b) Approximation of degradation cost: For our degradation model, we assume the internal resistance to be constant $R_{\text{int}} = 2.5\ \text{m}\Omega$ within 20% to 80% SOC range and under moderate range of temperature (See Section II B-e). With simple assumption, we derive tractable convex surrogate cost function $J_{\text{degrad}}^{\{\alpha\}}$ using Least Square with fitting parameters $\alpha \in \mathbf{R}^3$ where $\alpha = (\alpha_1, \alpha_2, \alpha_3)$ as

$$J_{\text{degrad}}^{\{\alpha\}} = \int_{t=0}^{T} \left(\alpha_1 |P_b(t)| + \alpha_2 T_b(t) + \alpha_3 \int_{\tau=0}^{t} |P_b(\tau)| d\tau \right) dt \tag{17}$$

where $\alpha_1 \ge 0$ and $\alpha_2 \le 0$. The sign of α_3 depends on type of battery, and here $\alpha_3 \le 0$ for the choice of $z = 0.5$. See the details on how to fit over data in Appendix V-D. Using these approximations, the problem transforms to a mixed-integer convex optimization which can find the global solution using standard methods such as branch-and-bound and interior point method [17].

IV. Results and Analysis

A. Experiment Setting

a) Computation: We show that our formulation (15) can be efficiently solved in Julia (with package `Convex.jl` [18]) within a minute (on 2.6 GHz Intel Core i7 processor), which is fast enough to be computed in real time. We discretize all continuous time terms with Δt interval in order to compute integrals and solution approximately.

b) Simulator: The model in Section 3 is a simplified model which can be run in real time.[1] The optimal controller takes the simulated data and produces the optimal strategy based on our simplified model. To test the results from the optimal controller, we use Autonomie, a vehicle simulator developed by Argonne National Laboratory which has been studied and verified against various kinds of vehicles [1]. Since our work focuses on a PHEV model with two modes, we consider a vehicle which has specifications close to that of Toyota Prius. For detailed parameters of our vehicle and the cooling system, refer to our previous work [2] and Table II.

c) Routes with Power Demand: We use six synthetic routes to test the efficiency of controllers where each route contains two different regions: one represents a highway region with constant speed cruise and the other represents an urban region with numerous start-stop cycles and speed variations including zero speed intervals. These routes have three different cruise speeds: 1) medium speed (39 mph), 2)

[1]The code and simulator is available at `https://github.com/jkim22/battDegradOpt_code.git`

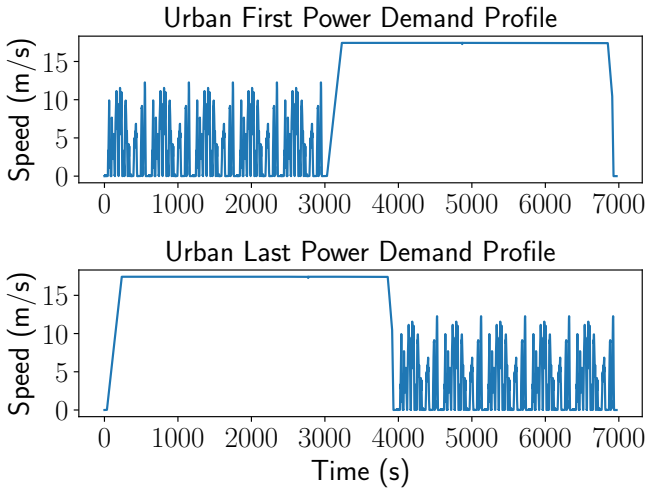

Fig. 1: Two power domain profile (P_{des}) examples, consisting of an urban region and a suburban cruise region but with order interchanged. Cruise region requires constant medium speed of 39 mph (17.5 m/s).

medfast speed (65 mph) and 3) fast speed (85 mph). Figure 1 represents two different routes with medium speed cruise component but with the the suburban and urban regions inverted in order.

In our earlier related work [2], we observe that even though the total power demand is the same for the mixed urban-suburban routes with order interchanged, the amount of fuel consumption varies depending on the control strategy employed by PHEVs. Here, we extend this observation to include battery degradation and see how battery thermal model and degradation model affects strategies of the optimal controller over various routes.

d) Weight Parameters: The objective of our optimization problem (15) is formed by the weighted sum of four objectives. Weights λ_1, λ_2 and λ_3 quantifies the importance of J_{cooling}, J_{degrad} and S respectively. Since our focus is on degradation model rather than power usage of cooling system, we set $\lambda_1 = 1$ for all cases. Also, we set $\lambda_3 = 20,000$ to encourage a realistic total number for the engine on/off switching. While fixing other weight parameters, we tune the parameter λ_2 to test our controller with appropriate battery degradation considerations. The value of J_{degrad} is not comparable to other objectives so it is important to adjust λ_2 to achieve efficient control strategy. For more sophisticated approach, we can incorporate λ_2 which reflects real economic cost ratio between fuel price and battery price, but here we use a simpler approach and defer this analysis to the longer version of our paper. For an effective hyper-parameter search, we normalize degradation parameters $\{\alpha\}$ (multiplying $\sum_{i=1}^{3} \alpha_i$ to λ_2). Also, we test the effect of λ_2 by solving the problem (15) under different choices of λ_2.

e) Different Ambient Temperatures: The battery degradation model (17) depends on battery temperature T_b and it is mainly controlled by the cooling system (12) which aims to keep the T_b based on ambient temperature setting. Therefore, we test the effect of various ambient temperature settings

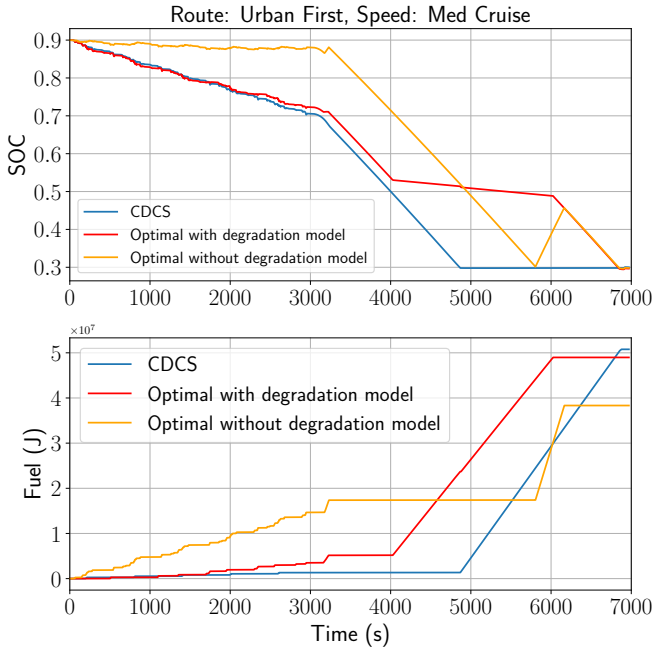

Fig. 2: Comparison of SOC and total fuel use of our controller (red) and baselines (blue, orange) after one cycle.

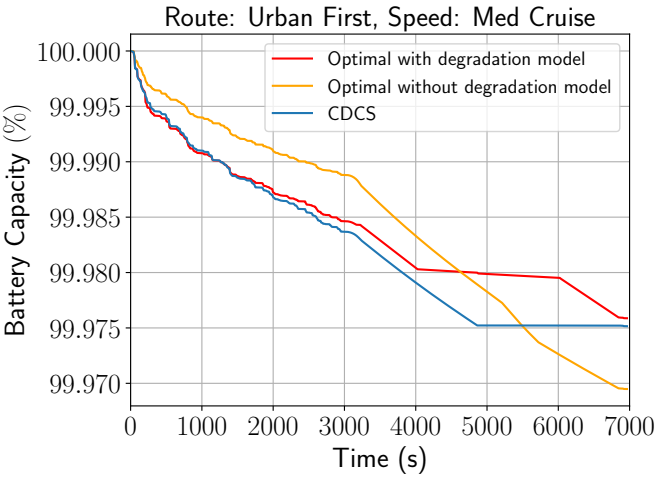

Fig. 3: Comparison of battery capacities remained over our controller (red) and baselines (blue, orange) after one cycle.

under fixed weight parameters of our optimal controller. The temperature is ranging from 298K to 320K which represents the room temperature to relatively hot temperature.

f) Baselines: We compare our optimal controller with two baselines: CDCS controller and the controller on our earlier related work [2]. CDCS uses a simple strategy which preferentially uses battery first and then uses the fuel resources and engine for operation. The other controller aims to minimize the total fuel usage and the number of drivetrain switching modes. We simulate the synthetic routes under these three controllers and compare the performances.

B. Analysis

a) Balancing Resources and Battery Degradation over Different Routes: We tested our optimal controller on six

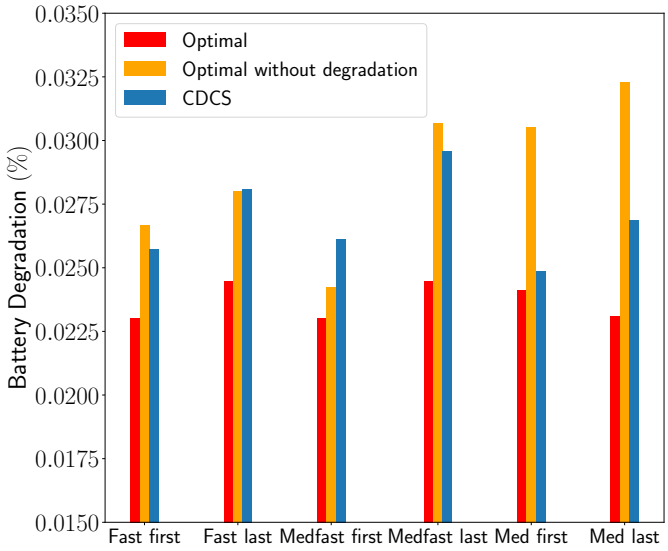

Fig. 4: Comparison of battery degradation, *i.e.*, Q_d, over six different routes after one drive cycle.

different synthetic routes with known power demand profiles and compared with two baselines. Figure 2 shows the battery SOC and combustion fuel use over time for a route with an urban region first and then suburban region with a medium speed cruise. Although all controllers start and end with same battery SOC, fuel consumption varies over the same route. The main difference is in the cruise component (approximately from time 3200 seconds) where our controller shows steady but smaller usage of battery energy compared to other controllers. As expected, optimal control without degradation shows significantly less fuel consumption compared with other controllers while it results in the most battery degradation as Figure 3 suggests. This result shows that the high currents used by the earlier controller, while achieving minimums of fuel use, can affect the battery longevity.

Overall our optimal controller showed less degradation compared to other controllers over the routes we tested (Figure 4). The result is based on driving each route at exactly once and on average, our controller obtains 12% less battery degradation than that of CDCS. Also, our controller is able to maintain 17.5% more battery capacity than that of the other baseline controller. Based on these results, we can estimate how much the battery capacity (or life) would degrade after three years, assuming this trip is daily. Our controller is estimated to suffer battery capacity degradation about 16% at most while other two baselines suffer 20% or more battery capacity loss (See Figure 8 and 9 in Appendix for the detailed comparisons). These results emphasize that the control method is capable of balancing the efficiency between fuel and battery resources. For practical economic reasons, extending the battery lifetime is of significant value to the vehicle owner and manufacturer.

b) The Effect of Degradation Weight Parameters: Figure 5a shows the result on a route consisting of an urban region followed by the suburban region with medium speed cruise. It shows that increasing λ_2 weight encourages the

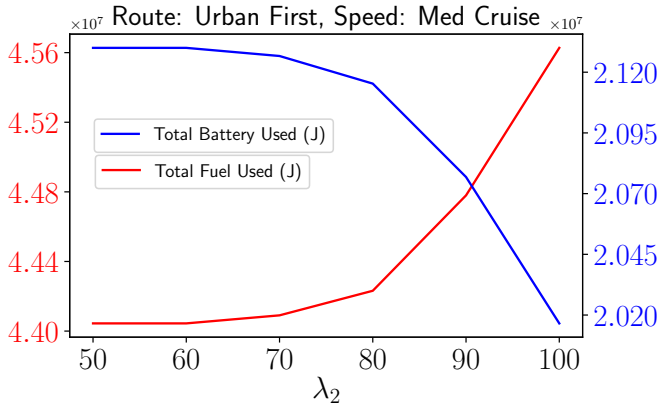

(a) The effect of using different λ_2 for the optimal control. As λ_2 increases, use fuel more and battery less.

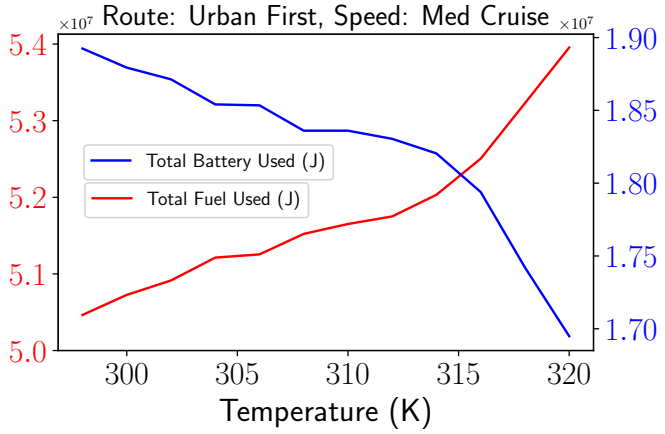

(b) The effect of different T_{amb} for the optimal control. In higher T_{amb}, more J_{fuel} used.

Fig. 5: Result on using different λ_2 and T_{amb}.

controller to use more fuel while discouraging battery usage.

c) The Operation on Various Ambient Temperatures: Under fixed λ_1, λ_2 and λ_3, we tested various ambient temperatures, ranging from 298K (*i.e.*, ambient temperature) to 320K (*i.e.*, hot weather). Overall, higher ambient temperature resulted in more total fuel usage and less battery power (See Figure 5b).

V. Conclusion

We have proposed an efficient control method which balances the fuel and battery resources while taking battery degradation into consideration over the predetermined route. To do so, we integrated a battery thermal model and battery degradation model into our problem. This extends the capability of the battery degradation control, beyond that of CDCS or other controllers designed to minimize fuel resources only. We posed a mixed-integer convex optimization problem and showed that our controller is capable of generating a tractable control strategy which is fast (efficient) enough to be computed on the on-board vehicle computer.

This technique is readily applicable in current vehicles as well as any hybrid vehicle in the future that manages fuel and battery resources during operation. Expanding the work to incorporate route estimation methods to the unknown route

setting is an interesting future direction. Another future extension for more practical purpose is developing the control method of power splitting over multiple resources, beyond one fuel engine and one battery, to allow energy management with supercapacitors over diverse real-world routes.

ACKNOWLEDGMENT

We would like to acknowledge contributions and support from J. Platt and N. Moehle and appreciate support from the Stanford-Ford Alliance program at Stanford University. We also thank Dyche Anderson, Rajit Johri, Ming Kuang, Connie Qiu, Ming Cheng from Ford for useful discussion and feedback.

REFERENCES

[1] Argonne National Laboratory, *Autonomie User Guide*, 2018.
[2] J. Platt, N. Moehle, J. D. Fox, and W. Dally, "Optimal operation of a plug-in hybrid vehicle," *IEEE Transactions on Vehicular Technology*, vol. 67, no. 11, pp. 10366–10377, 2018.
[3] J. Heywood and D. MacKenzie, "On the road toward 2050: Potential for substantial reductions in light-duty vehicle energy use and greenhouse gas emissions," tech. rep., MIT Energy Initiative Report, 2015.
[4] H. Helms, M. Pehnt, U. Lambrecht, and A. Liebich, "Electric vehicle and plug-in hybrid energy efficiency and life cycle emissions," *18th International Symposium Transport and Air Pollution*, 01 2010.
[5] I. Chung, H. Kang, J. Park, and J. Lee, "Fuel economy improvement analysis of hybrid electric vehicle," *International Journal of Automotive Technology*, vol. 20, pp. 531–537, Jun 2019.
[6] S. Moura, H. Fathy, D. Callaway, and J. Stein, "A stochastic optimal control approach for power management in plug-in hybrid electric vehicles," *Control Systems Technology, IEEE Transactions on*, vol. 19, pp. 545 – 555, 06 2011.
[7] P. Tulpule, V. Marano, and G. Rizzoni, "Effects of different phev control strategies on vehicle performance," in *2009 American Control Conference*, pp. 3950–3955, June 2009.
[8] A. Samba, *Battery electrical vehicles analysis of thermal modelling and thermal management*. PhD thesis, LUSAC (Laboratoire Universitaire des Sciences Appliquées de Cherbourg), 2015.
[9] E. Sarasketa-Zabala, I. Gandiaga, L. Rodríguez-Martínez, and I. Villarreal, "Calendar ageing analysis of a lifepo4/graphite cell with dynamic model validations: Towards realistic lifetime predictions," *Journal of Power Sources*, vol. 272, p. 45–57, 12 2014.
[10] X. Gong, "Modeling of lithium-ion battery considering temperature and aging uncertainties," in *Deep Blue*, University of Michigan-Dearborn, 2016.
[11] J. Wang, P. Liu, J. Hicks-Garner, E. Sherman, S. Soukiazian, M. Verbrugge, H. Tataria, J. Musser, and P. Finamore, "Cycle-life model for graphite-lifepo 4 cells," *Lancet*, vol. 196, pp. 3942–3948, 04 2011.
[12] N. H. F. Ismail, S. F. Toha, N. A. M. Azubir, N. H. M. Ishak, M. K. Hassan, and B. S. K. Ibrahim, "Simplified heat generation model for lithium ion battery used in electric vehicle," *IOP Conference Series: Materials Science and Engineering*, vol. 53, p. 012014, dec 2013.
[13] A. Ahmadian, M. Sedghi, A. Elkamel, M. Fowler, and M. Aliakbar Golkar, "Plug-in electric vehicle batteries degradation modeling for smart grid studies: Review, assessment and conceptual framework," *Renewable and Sustainable Energy Reviews*, 06 2017.
[14] "What causes li-ion to die?," *Battery University*, 2017.
[15] H. Ibrahim, A. Ilinca, and J. Perron, "Energy storage systems—characteristics and comparisons," *Renewable and Sustainable Energy Reviews*, pp. 1221–1250, 06 2008.
[16] J. P. R., A. Pesaran, and K. Smith, "Electric vehicle battery thermal issues and thermal management techniques." SAE 2011 Symposium, 2011.
[17] S. Boyd and L. Vandenberghe, *Convex Optimization*. New York, NY, USA: Cambridge University Press, 2004.
[18] M. Udell, K. Mohan, D. Zeng, J. Hong, S. Diamond, and S. Boyd, "Convex optimization in julia," in *Proceedings of the 1st First Workshop for High Performance Technical Computing in Dynamic Languages*, pp. 18–28, IEEE Press, 2014.

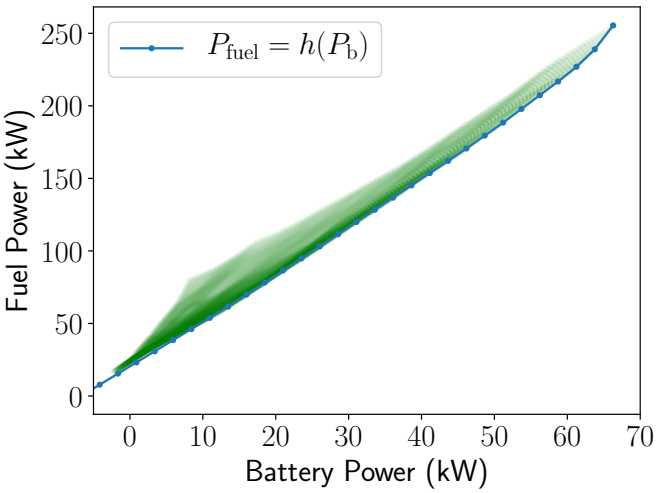

Fig. 6: Function $P_{\text{fuel}} = h(P_{\text{b}})$ for a power split hybrid for a given P_{des} and wheel speed w

APPENDIX

A. Gridding Technique

In this section, we show our method on representing the $h : \mathbf{R} \mapsto \mathbf{R}$ in a tractable form. Firstly, based on given vehicle configurations, we calculate upper/lower bounds of the control inputs (*e.g.*, engine speed Ω, engine torques, τ). Next, for fixed P_{des}, wheel speed w and engine on/off θ, we consider all of these configurations to obtain corresponding P_{b} and P_{fuel}. The interpretation is that we consider all convex combinations of internal configurations for a particular known P_{des}, w and θ. Then, we find the best convex function h that best fits on all points (P_{fuel}, P_b) (See Figure 6). For example, when $\theta = 0$ in our power-split PHEV model case, engine is off so all the power comes from the battery (*i.e.*$P_{\text{des}} = P_b$). For $\theta = 1$ case, engine is on so we consider all points (P_{fuel}, P_b) and find the best (approximated) function h.

B. Parameters

Our battery heat transfer model used following parameters as shown in table II. We set $T_{\text{amb}} = 298K$, $T^{\min} = 290K$, $T^{\max} = 343K$, $E^{\min} = 1 \times 10^7$ Joules, $E^{\max} = 2.5 \times 10^8$ Joules. Note that the current Plug-in Hybrid Prius configuration has battery mass of 80 kg (180 lb) and battery capacity of 8.8 kWh. Our model is roughly similar to Prius, the existing commercial PHEV.

Parameters	Model	Unit
Battery Mass (m)	70.62	kg
Heat Capacity (C)	795	$J/kg \cdot K$
h_{trans}	137.5	$W \cdot m^{-2} \cdot K$
$P_b^{\max}$	30000	W
$P_b^{\min}$	-20000	W
Battery Capacity	7.8	$k \cdot Wh$

TABLE II: Parameters for Battery Thermal Model

C. Additional Results

a) Different routes: In some cases, our optimal controller generated a strategy with more fuel consumption than

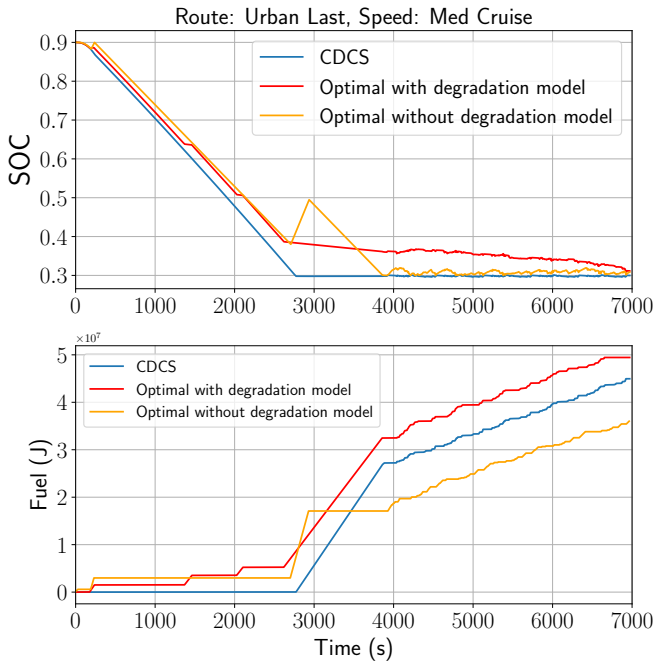

(a) Comparison of battery state-of-charge and total fuel use of our controller (red) and baselines (blue, orange). λ_2 is set to 70.

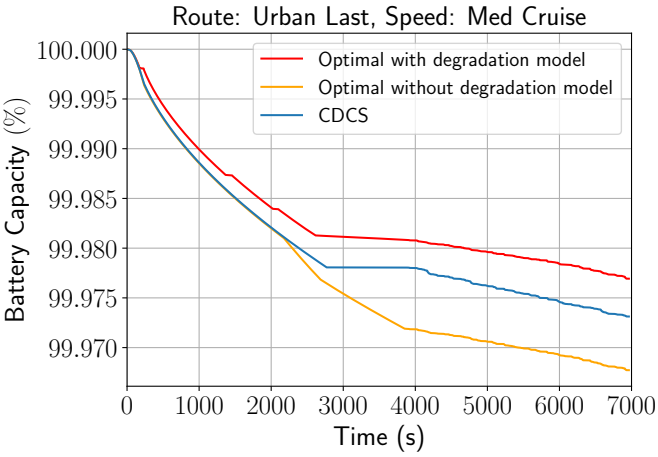

(b) Comparison of battery capacities remained over our controller (red) and baselines (blue, orange) after one cycle.

Fig. 7: Result on Urban Last Route

other controllers. For example, in Figure 7a and 7b, our controller used significantly more fuel resources than those of two baselines. In this case, our controller decides to consume more fuel than battery resource to alleviate future battery degradation effects.

b) Long term battery degradation effects: Figure 8 and 9 shows degradation of battery capacity after one year and three years respectively. In all cases, our controller suffers less battery degradation then that of other two baselines.

D. Least Square to Fit Degradation Cost

Note that $\sqrt{|P_b(t)|} \propto |I(t)|$ because the internal resistance, R_{int} can be approximated by a constant (≈ 2.5 mΩ). Therefore, we use $P_b(t)$ as a variable in Q_d. We assume $\phi(x) = \log(x+1)$ which is nonnegative for $x \geq 0$ and increasing.

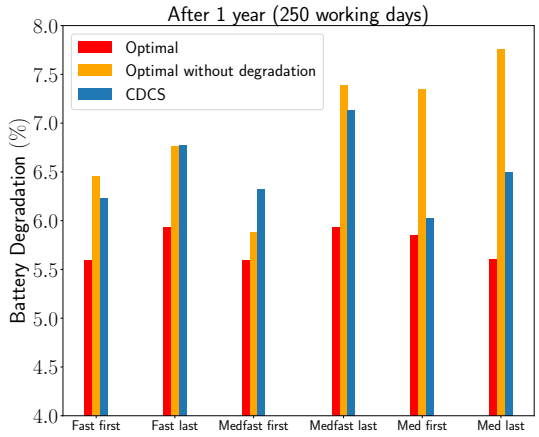

Fig. 8: Comparison of estimated battery degradation, *i.e.*, Q_d, over six different routes for one year (250 route trips)

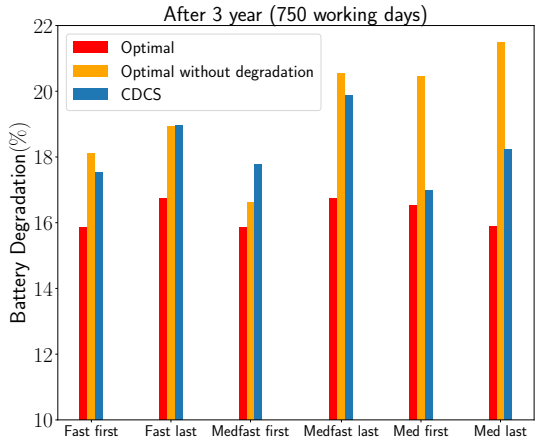

Fig. 9: Comparison of estimated battery degradation, *i.e.*, Q_d, over six different routes for three years (750 route trips)

$$\log\left(\dot{Q}_d(t)+1\right) = \log(c_1) + \frac{c_2 + c_3|I_b(t)|}{R_{\text{gas}}T_b(t)} - \frac{1}{2}\log Ah_t + \frac{1}{2}\log|I_b(t)|,$$

implying $\log\left(\dot{Q}_d(t)+1\right)$ is proportional to $|P_b(t)|$ and inversely proportional to $T_b(t)$ and $\int_{\tau=0}^{t}|P_b(\tau)|d\tau$.

Then we approximate this cost function. To achieve a tractable convex battery degradation model, we adopt a data efficient method which is to calculate Q_d based on our available route data $D \in \mathscr{D}$ and fit the model best using a least square method. In other words, we solve

$$\min \sum_{D\in\mathscr{D}} \int_{t=0}^{T} \Big(\| \log(Q_d^D(t)+1) - \alpha_1 P_b^D(t) - \alpha_2 T_b^D(t) - \alpha_3 \int_{t'=0}^{t} P_b^D(t')dt' \|_2^2 \Big) dt$$

with variables α_1, α_2 and $\alpha_3 \in \mathbf{R}$. Then, we obtain a tractable degradation cost function as

$$J_{\text{degrad}}^{\{\alpha\}} = \int_{t=0}^{T} \left(\alpha_1 P_b(t) + \alpha_2 T_b(t) + \alpha_3 \int_{t'=0}^{t} P_b(t')dt' \right) dt.$$